RSC Advances

ROYAL SOCIETY OF CHEMISTRY

www.rsc.org/advances

Journal Name

ARTICLE

A Novel g-C_3N_4 Based Photocathode for Photoelectrochemical Hydrogen Evolution

Received 00th January 20xx,
Accepted 00th January 20xx

DOI: 10.1039/x0xx00000x

www.rsc.org/

Yuming Dong,*[a] Yanmei Chen,[a] Pingping Jiang,[a] Guangli Wang,[a] Xiuming Wu[a] and Ruixian Wu[a]

Nowadays, the fabrication of photocathodes with high light-harvesting capability and charge transfer efficiency is a key challenge for photoelectrochemical (PEC) water splitting. In this paper, a novel graphitic carbon nitride (g-C_3N_4) based photocathode was designed, prepared and used as photocathode for hydrogen generation from water. Here we employed g-C_3N_4 as a photosensitizer and co-catalyst for photoelectrochemical hydrogen evolution for the first time. The g-C_3N_4 based photocathode exhibited superior light absorbance and excellent photoactivity. Under irradiation, the photocurrent response of the g-C_3N_4/NiO photocathode at a bias potential of 0 vs RHE is approximately ten times as that of the NiO photoelectrode and twenty times as that of the g-C_3N_4 photoelectrode. And the g-C_3N_4/NiO photocathode has excellent activity for hydrogen production with nearly 100% faraday efficiency without external co-catalyst and buffer solution. Moreover, the g-C_3N_4/NiO photoelectrode showed superior stability both in nitrogen-saturated and air-saturated neutral environment.

1. Introduction

Over the past few decades, energy and environment issues have become one of the most important and popular subjects at a global level.[1] Compared with fossil fuels, hydrogen energy as an environmentally benign fuel has higher calorific value, which is almost four times higher than that of methane.[2,3] Production of hydrogen from water has been attracting a lot of attention because of the possibility of generating a clean energy carrier without CO_2 emissions, as well as opportunities in the field of energy storage.[4] Photoelectrochemical (PEC) water splitting is the one of highly promising methods to produce hydrogen, which captures and stores solar energy in the simplest chemical bond (H_2), without any undesired pollutants.[5,6] In general, PEC devices are composed of two different photoelectrodes, photocathode and photoanode, where reduction and oxidation of water occurs with response to sunlight. Whether the photoanode or photocathode generally consistses of three components, n-semiconductor or p-semiconductor, photosensitizer and co-catalyst.

In a PEC electrode, the light absorber is the key component that needs to sensitize a wide band gap semiconductor and is also coupled with a co-catalyst to drive the production of chemicals at the electrode. The organic dyes, firstly appeared photosensitizer, suffer from easily degrading for sensitized photoelectrodes due to the desorption of dye molecules[7] or the leaching of catalysts.[8,9] Subsequently, cadmium chalcogenide perfectly replace organic dyes with appropriate band gap that can make use of the full spectrum of sunlight, easy fabrication, large scale reducibility, a tunable light absorption spectrum through varying particle size and possible multiple exciton generation.[10] However, the toxicity and non-abundant content of the cadmium element in cadmium chalcogenide[11,12] limit their wide uses.[13] Therefore, the development of a novel, non-toxic, low prices, efficient and stable light absorber is of great significance. In addition, in order to accelerate electron transfer, reduce the recombination of electrons and holes and improve the efficiency of hydrogen production, certain co-catalyst is essential.

As a metal-free photocatalyst, graphitic carbon nitride (g-C_3N_4) has attracted intensive interest for its promising applications in splitting water to produce H_2,[14] decomposition of organic pollutants,[15] and organic synthesis under light.[16] The g-C_3N_4 has a moderate band gap (2.7 eV) and consequently can absorb light up to 450 nm. Besides, g-C_3N_4 possesses high chemical and thermal stability as well as fascinating electronic property.[17] In photocatalytic hydrogen production, lots of photocatalysts based on g-C_3N_4 with various morphologies have been synthesized and exhibited excellent photoactivity for H_2 generation.[18-34] Recently, Shalom *et al*. presented a highly ordered carbon nitride on different substrates as electrocatalysts show high activity in the HER with low overpotential and acceptable current densities.[4] Duan *et al*. fabricate such a 3D hybrid film by integrating intentionally 2D porous g-C_3N_4 nanolayers with N-doped graphene sheets (denoted as PCN@-N-graphene film), which exhibits a superior HER catalytic activity with a low overpotential.[35] In summary, g-C_3N_4 can not only be used as a photosensitizer but also could enhance the reactivity as a co-catalyst in PEC hydrogen production. However, PEC studies involving g-C_3N_4-sensitized photoelectrodes[36,37] are scarcely studied to date. Take this into account, we proceed on the design of g-C_3N_4 sensitized photocathode for H_2 envolution in water. Nickel oxide as a p-type semiconductor, has been identified to be an excellent platform for hole conduction.[38-40] We imagine that g-C_3N_4 has the ability to inject holes into NiO for fabricating a photocathode. That's because g-C_3N_4 has a more positive valence band potential than NiO.[41]

[a] Key Laboratory of Food Colloids and Biotechnology (Ministry of Education of China), School of Chemical and Material Engineering, Jiangnan University, Wuxi 214122, P. R. China

† Electronic Supplementary Information (ESI) available: [details of any supplementary information available should be included here]. See DOI: 10.1039/x0xx00000x

* Corresponding author. Fax: +86 510 85917763. E-mail address: dongym@jiangnan.edu.cn (Y. Dong).

Recently, a hybrid NiO–g-C_3N_4 photocatalyst for efficient methylene blue degradation has been reported.[42] And the improved photoactivity of NiO–g-C_3N_4 photocatalysts could be ascribed to the effective interfacial charge transfer between NiO and g-C_3N_4. Appreciated from the foregoing, the combination of NiO and g-C_3N_4 may be an excellent system to achieve enhanced PEC properties. As know, no report about the coupling of NiO and g-C_3N_4 as a photocathode for H_2 envolution has been reported. In this research, we prepared NiO by hydrothermal process, and then coupling the g-C_3N_4 with NiO with a facile thermal polycondenzation method (Scheme S1). Under illumination, the prepared g-C_3N_4/NiO photoelectrode achieved the highest photocurrent density at a bias potential of 0 vs RHE, which is approximately ten times as that of the NiO photoelectrode and twenty times as that of the g-C_3N_4 photoelectrode. Furthermore, charge transfer property was investigated by photoluminescence (PL) analysis and electrochemical impedance spectroscopy (EIS). The possible mechanism for enhancement of the PEC properties was also discussed.

2. Experimental section

2.1. Materials

Hexamethylenetetramine ($C_6H_{12}N_4$), nickel (II) nitrate hexahydrate ($Ni(NO_3)_2·6H_2O$), thiourea, potassium chloride (KCl), hydrochloric acid (HCl), sodium sulfate, ethanol, acetone and deionized water. All of the materials were analytical grade and used as received without further purification.

2.2. Preparation of Photocathode

Preparation of NiO/FTO electrode. The NiO/FTO electrode was prepared according to our previous report.[45] The fabrication was described briefly as follows: the FTO glass was placed in a mixed aqueous solution, which contains 0.25 mol/L nickel(II) nitrate hexahydrate and 0.25 mol/L hexamethylenetetramine, heated at 100 °C for 12 min, then taken out and cleaned thoroughly with deionized water and dried. Finally the as-fabricated FTO glass was annealed at 450 °C in muffle furnace for 2 h.

Preparation of g-C_3N_4/NiO/FTO electrode. The pristine g-C_3N_4/NiO/FTO electrode obtained by simply heating thiourea/NiO/FTO at 500 °C for 2 h under N_2 gas flowing. In detail, the electrode was prepared as follows: firstly, the NiO/FTO electrode was immersed in a saturated aqueous solution of thiourea for 4 h; then, the thiourea/NiO/FTO was sintered under a gentle N_2 flow at 500 °C for 2 h using an alumina boat.

Preparation of g-C_3N_4/FTO electrode. The pure g-C_3N_4 sample was prepared under same conditions for g-C_3N_4/NiO/FTO electrode, using thiourea as the raw material. Briefly, thiourea was placed in a porcelain boat and heated at 500 °C for 2 h under N_2 atmosphere. The yellow bulk g-C_3N_4 was obtained and can be used after being grinded. Deposition of g-C_3N_4 onto the FTO was conducted by an electrophoresis process. 10 mg g-C_3N_4 was added into isopropanol (100 mL) with sonication dispersion for 3 h and then 10 mg $Mg(NO_3)_2·6H_2O$ was added into above suspension with ultrasonic dispersion for another 1 h. In succession, FTO as a cathode and Pt wire as an anode were immersed in the stable suspension with a distance of 1 cm. Then the electrophoretic deposition was performed at 160 V for 1 min.

2.3. Characterization

The size and surface morphologies of the sample were investigated by field emission scanning electron microscopy (FE-SEM) on a Hitachi S-4800 and transmission electron microscopy (TEM) on a JEM-2100 transmission electron microscope (JEOL, Japan). To identify the composition and phase of sample, powder X-ray diffraction (XRD) patterns were collected using a Bruker-AXS D8 advance diffractometer with Cu Kα radiation. The ultraviolet-visible absorption spectra were recorded using a UV-1800 spectrometer (Meipuda Instruments Co. Shanghai). To detect the chemical composition and electronic structure of sample, X-ray photoelectron spectroscopy (XPS) analysis was conducted using an ESCALAB 250 Xi (Thermo, USA) X-ray photoelectron spectrometer with Al Kα line as the excitation source (hv = 1484.6 eV) and adventitious carbon (284.6 eV for binding energy) was used as reference to correct the binding energy of sample.

2.4. Photoelectrochemical Measurements

Electrochemical measurements were performed on a CHI 660E electrochemical instrument (Chenhua Instruments Co. Shanghai) with a standard three-electrode system. The prepared electrodes act as working electrodes, using a Pt wire and Ag/AgCl (3M KCl) as counter electrode and reference electrode, respectively. The light source utilizes a 300 W Xe arc lamp and the average power density was 245 mW/cm^2. The electrolyte was Na_2SO_4 aqueous solution. This electrolyte solution was used for all experiments unless otherwise mentioned. The three-electrode system and electrolyte were then degassed using a mixture of 20% CH_4 in N_2 with the CH_4 being used later as an internal reference for GC analysis. The amount of H_2 evolved was determined with an gas chromatography (GC-9790) equipped with a thermal conductivity detector (TCD). The electric potential is calculated as follows：

$$E\ (V\ vs\ RHE) = E(vs\ Ag/AgCl) + 0.208 + 0.059pH$$

3. Results and discussion

3.1. Structure and morphology characterization of g-C_3N_4/NiO/FTO

In order to obtain the microscopic structures of g-C_3N_4/NiO and blank NiO on FTO, we carried out SEM analyses. The morphological changes of the NiO structure upon subsequent deposition of g-C_3N_4 as shown in Figure 1(a) and 1(b), reveal that some g-C_3N_4 nanosheets attached onto the surface of NiO porous honeycomb structure. It is noted that some g-C_3N_4 nanosheets were also filled in the NiO porous structure. After the g-C_3N_4 deposition, the surface of the NiO eletrode appears to be tight and uniform, and disperses evenly over the whole NiO substrate. Fig. 1(c) shows the TEM image of the powder scraped from the g-C_3N_4/NiO film coated on the FTO substrate. It can be found that the nanosheet morphology existed in the g-C_3N_4/NiO composite powder, which should be

Journal Name

ARTICLE

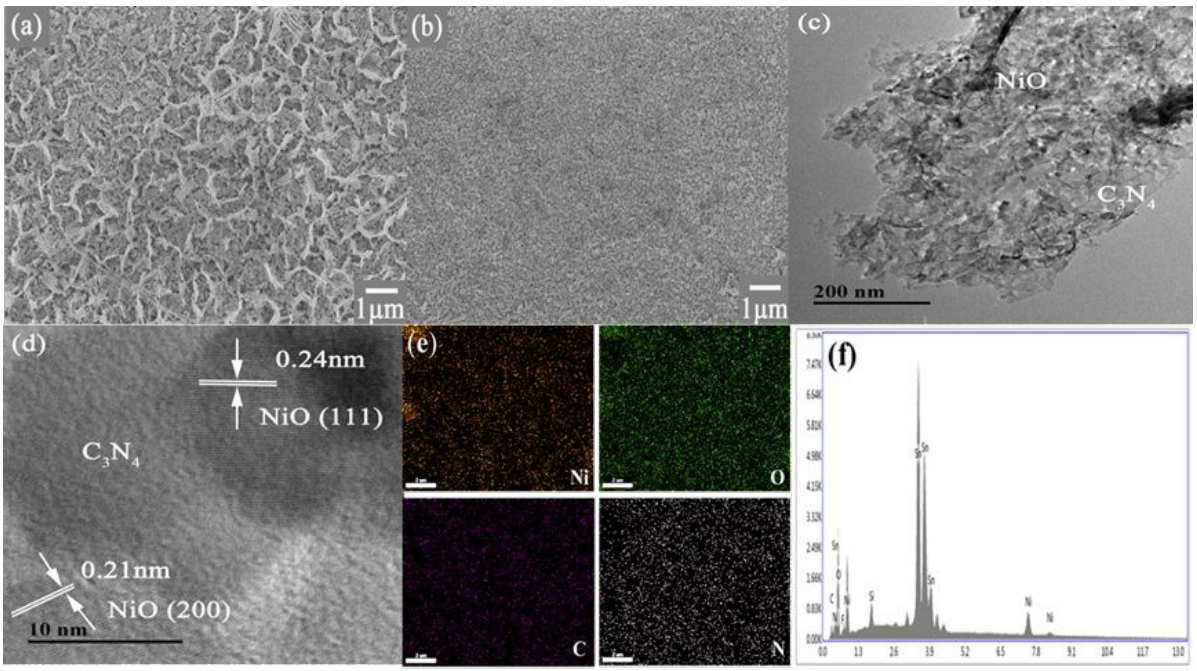

Figure 1. (a) SEM image of NiO/FTO; (b) SEM, (c) TEM, and (d) HRTEM images of g-C_3N_4/NiO/FTO; (e) energy-filtered elemental mapping image and (f) EDX spectrum of g-C_3N_4/NiO/FTO.

considered as the polymeric g-C_3N_4. The HRTEM image of g-C_3N_4/NiO composite film (Fig. 1(d)) also shows some lattice fringes of NiO can be observed on top of those of g-C_3N_4. The d spacing of 0.24 nm and 0.21 nm can be assigned to the (111) and (200) facets of NiO. In addition, the EDX spectrum confirms the co-existence of Ni, O, C and N (Fig. 1(f)); and the energy dispersive X-ray spectroscopy (EDS) elemental mapping of Ni (yellow), O (green), C (purple) and N (white) displayed in Figure 1(e) suggests a good dispersion of NiO and g-C_3N_4 on the surface of FTO.

XRD technique was used to determine the crystalline features of as-prepared electrodes. Figure S1 shows the XRD patterns for the NiO/FTO electrode and g-C_3N_4/NiO/FTO electrode before and after the reaction, respectively. For all the samples, the diffraction peaks at 26.6 (110), 37.9 (200), 51.8 (211), 61.9 (310), 66.0 (301), and 81.2 (400) are attributed to the rutile SnO_2 phase (JCPDS No. 21-1205) of the FTO substrate. No characteristic diffraction peaks of NiO and g-C_3N_4 were observed for the composite films because of their low content and poor crystallization. Furthermore, we carried out the XRD patterns of the pure g-C_3N_4 powder which was prepared under the same conditions as that on NiO/FTO. As shown in Figure S2, two pronounced diffraction peaks are found at 27.4° and 13.0° for g-C_3N_4 nanosheets, corresponding to the characteristic interlayer stacking peak of aromatic systems (indexed for graphitic materials as the 002 peak), and the interplanar separation (indexed as the 100 peak), respectively, which is consistent with the XRD pattern reported in the literature.[24,25,27,36,37,43] The results indicated that g-C_3N_4 did form under this experimental conditions.

The composition and element valence of the heterostructured films were investigated by X-ray photoelectron spectroscopy. The XPS survey scans of g-C_3N_4/NiO/FTO electrode indicate the existence of Ni, O, Sn, C, and N (Figure 2a). The Ni 2p X-ray photoelectron spectra of nickel oxide are shown in Fig. 2(b). The spectra can roughly be divided into two edges split by spin-orbit coupling, referred to as 2p1/2 (870-885 eV) and 2p3/2 (845-869 eV) edges, respectively.[44] As shown in Fig. 2(b), the presence of Ni 2p3/2 peak at 853.9 eV which is in agreement with the Ni 2p3/2 binding energy (BE) values of NiO reported in literatures[44,45] indicates that Ni exists in NiO form. The corresponding O 1s spectra are shown in Fig. 2(c). The presence of O 1s signal at 529.5 eV further confirms the presence of NiO phase. The other peak of O 1s signal can be attributed to the O from SnO_2.

The high-resolution XPS spectrum of C 1s provided in Fig. 2(d) can be divided into three peaks with binding energy values of 284.8, 286.6 and 288.1 eV, respectively. The peak located at 284.8 eV can be assigned to the C–C and/or adventitious carbon, and the peaks at 286.6 and 288.1 eV can be ascribed to the C–N–C and the C–$(N)_3$

Journal Name

ARTICLE

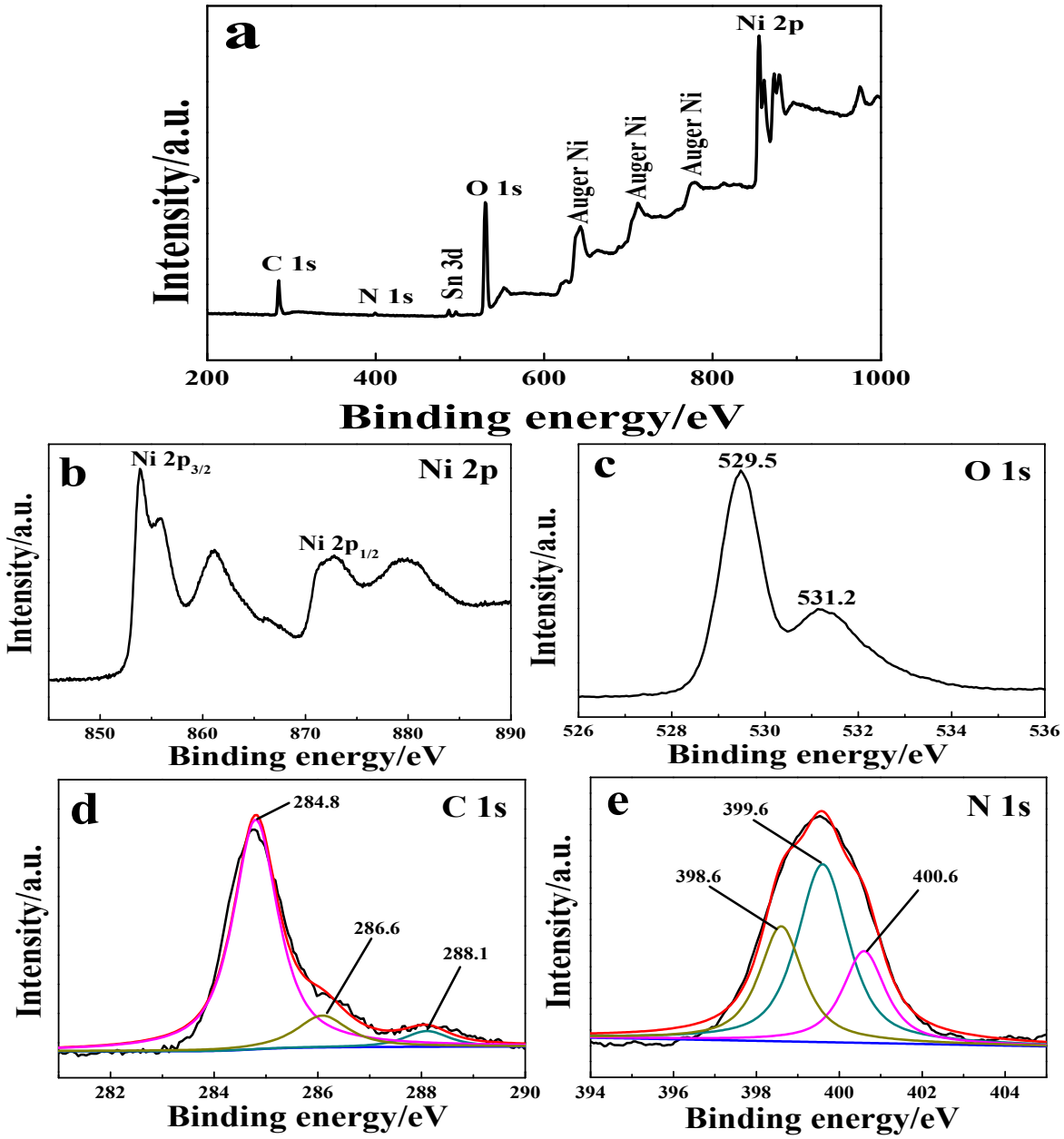

Figure 2. (a) Survey scan XPS spectra in the binding energy range 200-1000 eV and high-resolution spectra, (b) Ni2p, (c) O1s, (d) C1s and (e) N1s of g-C_3N_4/NiO.

group of g-C_3N_4,[24,27,33,35,37] respectively. The N1s high resolution spectrum in Fig. 2(e) can be fitted into three peaks. The peak 398.6 eV originates from the sp2-bonded N involved in the triazine rings, which dominates in g-C3N4, while the peaks at 399.6 and 400.6 eV indicate the presence of the tertiary nitrogen N–$(C)_3$ group and amino C–N–H.[21,32]

3.2. Photoelectrochemical properties

The optical absorption of the as-prepared g-C_3N_4 powder, NiO, and g-C_3N_4/NiO electrodes was measured using UV-vis diffuse reflectance spectroscopy after deducting the absorbance of FTO background. As presented in Fig. 3(a), the absorption edge of the pure g-C_3N_4 was around 440 nm, and the bandgap energy (E_g) was thus determined to be 2.85 eV by measuring the x-axis intercept of

an extrapolated line from the linear regime of the Tauc plot curve (Fig. 3A, the inset). Furthermore, the black line obtained from pristine NiO shows very weak absorption in the visible region, and the red line originating from g-C_3N_4/NiO shows strong absorption in 350-460 nm region. Therefore, it can be seen that the absorption peak of g-C_3N_4/NiO sample shifts significantly to longer wavelengths as compared to NiO, which implies that the absorbance of the electrode has been enhanced.

The photocurrent response measurement was carried out in a 0.10 M Na_2SO_4 electrolyte under irradiation using a 300 W Xenon lamp, to investigate the photo-induced charge separation and electronic interaction of g-C_3N_4 and NiO (Fig. 3(b)). It is clear that fast and uniform photocurrent responses can be obtained with the electrodes and the photoresponsive phenomenon is entirely reversible. The photocurrent density of the g-C_3N_4/NiO/FTO electrode is approximately 0.02 mA cm^{-2} at 0 V vs RHE, which is almost twenty times as that of g-C_3N_4/FTO and ten times as that of NiO/FTO (Fig. 3b). This result indicated that the combination of NiO and g-C_3N_4 was an ideal system to achieve enhanced PEC properties.

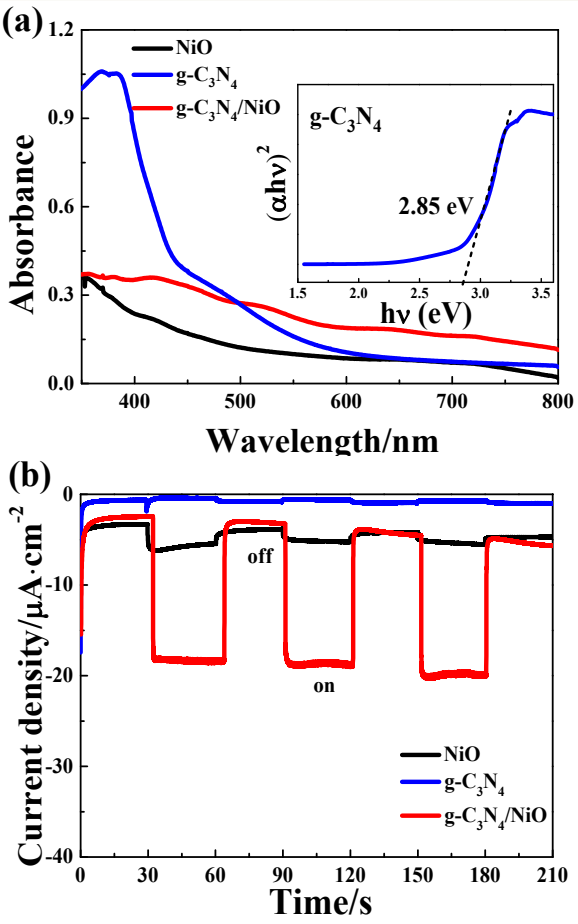

Figure 3. (a) UV-vis absorption spectra of g-C_3N_4 powder, NiO electrode and g-C_3N_4/NiO electrode; (b) Current density vs. time of the three electrodes under chopped light illumination in 0.10 M Na_2SO_4 solution at bias potential of 0 V vs. RHE. The inset in (a) is the Tauc plot providing the band gaps.

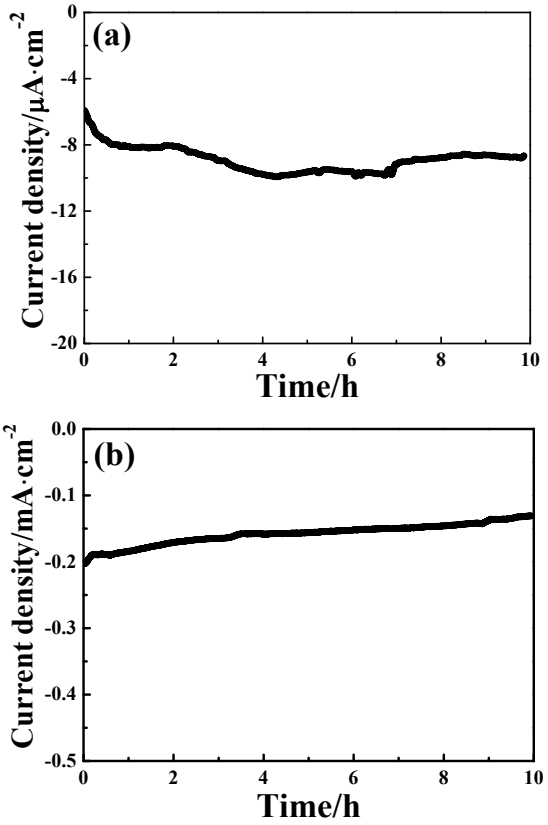

Figure 4. Charge-t and current-t curves of the g-C_3N_4/NiO/FTO electrode under illumination (a) at -0.2 V vs RHE in nitrogen saturated Na_2SO_4 (0.1mol/L) solution and (b) at 0 V vs RHE in air-saturated Na_2SO_4 (0.1mol/L) solution.

As known, the photochemical stability of the electrodes is very important for a PEC hydrogen generation system. Therefore, we measured the time dependence of the PEC performance. Fig. 4(a) and (b) demonstrate the photocurrent of the g-C_3N_4/NiO/FTO electrode along with time in nitrogen saturated electrolyte and air saturated electrolyte, respectively. We can see that the photocurrent density always maintained steady during 10 hours in both conditions. It is worth noting that a stable photocurrent density of 0.15 mA cm^{-2} was obtained in air saturated Na_2SO_4 solution. This value is considerably higher than that in nitrogen saturated electrolyte, because electrons could not only reduce the protons and also reduce the dissolved oxygen in the solution, resulting in the large photocurrent.[45] The results indicated that the g-C_3N_4/NiO/FTO electrode was highly stable either in the presence or in the absence of oxygen. Namely, the g-C_3N_4/NiO/FTO electrode can keep stable basically in many electrolyte solutions and conditions. In addition, we also studied current density-potential curves of the g-C_3N_4/NiO/FTO electrode through cyclic voltammetry for 200 cycles. As can be seen from Figure S3, the shape of the first cycle and the 200th cycle are identical and basically coincided. It can also prove the excellent stability of g-C_3N_4/NiO/FTO electrode. Therefore, a novel, non-toxic, low prices, efficient and stable photocathode was successfully prepared.

In order to show the influence of light and bias potential on PEC H_2 evolution rate, PEC control experiments of NiO/FTO, g-

C_3N_4/FTO and g-C_3N_4/NiO/FTO under irradiation (or not) and electrolysis (or not) were carried out and shown in Fig. 5(a). In the case of photocatalysis (without external voltage), the amounts of hydrogen production on all photoelectrodes were negligible for lack of electron source. In the case of electrocatalysis (without irradiation), the g-C_3N_4/NiO/FTO showed a low hydrogen generation rate while the NiO/FTO had a lower value and g-C_3N_4/FTO had almost no yield. In the presence of both visible light and bias potential, it can be clearly seen that the g-C_3N_4/NiO/FTO revealed higher activity with H_2 production rate of 0.16 μmol h^{-1} cm^{-2}, due to synergistic effect between g-C_3N_4 and NiO for charge transport. Furthermore, we compared the current density-potential curves of this electrode in light and no light conditions (Fig. 5(c)),found that the current density under light illumination was far greater than the value in the absence of light from -0.3 V to +0.3 V (vs RHE). The above results show that the electrode we prepared is an effective photocathode.

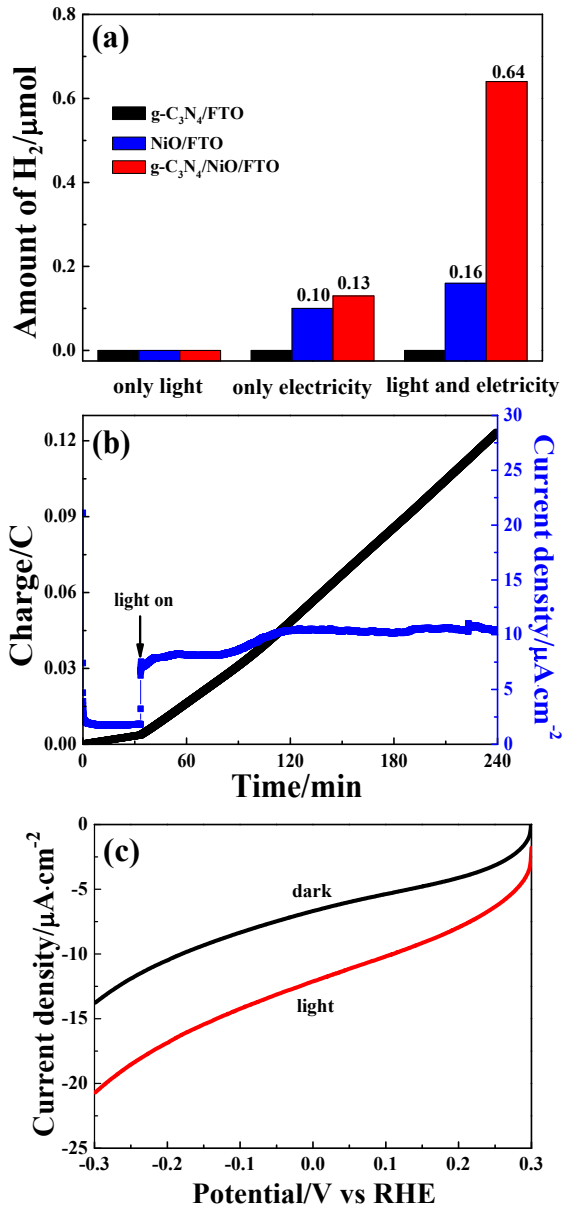

Figure 5. (a) Hydrogen evolution using NiO/FTO, g-C_3N_4/FTO and g-C_3N_4/NiO/FTO photocathodes 0.10 M Na_2SO_4 for 240 min under different conditions: only light (without bias potential), only electricity (at -0.2 V vs RHE without irradiation), light and electricity (at -0.2 V vs RHE with visible light irradiation); (b) Photocurrent density of the g-C_3N_4/NiO/FTO electrode in 0.10 M Na_2SO_4 solution under continuous irradiation at bias potential of -0.20 V vs. RHE; (c) current density-potential curves of g-C_3N_4/NiO/FTO electrode in N_2/CH_4 saturated 0.10 M Na_2SO_4 with light or dark.

To confirm the faradaic efficiency of PEC hydrogen evolu-tion using g-C_3N_4/NiO/FTO at E (vs RHE) = -0.2 V under irradiation, the charge and current along with time were recorded and shown in Fig. 5(b). During the experiment for 240 min, total charge passing through the electrode was 0.13 C, corresponding to 0.65 μmol assuming that all the electrons are used to produce H_2. The amount of H_2 (0.64 μmol) measured by gas chromatographic analysis of the head space, closely matched the number of electrons passed through the circuit. As controls, we have conducted the hydrogen production experiments on NiO/FTO and g-C_3N_4/FTO electrodes, and found that under the same conditions, the two electrodes can only produce a negligible amount of hydrogen gas. This demonstrates that the significant enhancement of PEC performance can be attributed to synergistic effect between g-C_3N_4 and NiO. In addition, at the begin of this experiment, when the light is off for 30 min, the current kept constant at 2 μA·cm^{-2}, and the photocurrent rises rapidly to 10 μA·cm^{-2} when the light was turned on. The results indicated the good light response of g-C_3N_4/NiO electrode in PEC hydrogen evolution. Then, the XRD data and XPS data on the sample after the test in Na_2SO_4 solution was characterized to confirm that materials is stable in the solution in Figure S1 and Figure S4. From the figure we can see there are no significant changes in XRD data and in the XPS data before and after the test in Na_2SO_4 solution, which indicates that materials we prepared is stable in the solution. Considering the results in Fig. 5 and Fig. S4 together, it can be considered that g-C_3N_4/NiO is an efficient and stable photocathode for PEC hydrogen production.

At last, we studied the practical use of our PEC system under natural sunlight outdoors. As be shown in Figure S5 and S6, there is a linear relationship between charge amount and time. That indicated the g-C_3N_4/NiO photocathode possessed excellent stability. During the experiment for 4 h, the total amount of H_2 measured by gas chromatographic analysis of the head space is 0.47 μmol. Considering the results, it can be considered that g-C_3N_4/NiO is also an efficient and stable photocathode for PEC hydrogen production with potential use under sunlight.

3.3. Proposed mechanism for the enhanced PEC properties

In the previous studies, photoluminescence (PL) analysis was used to reveal the efficiency of charge carrier trapping, transfer, and separation and to investigate the fate of photogenerated electrons and holes in semiconductors, because the PL emission results from the recombination of free charge carriers. Herein, we present the suitable PL measurement for NiO/FTO, g-C_3N_4/FTO and g-C_3N_4/NiO/FTO electrodes under photoexcitation at 325 nm, as shown in Figure 6(a). The emission peak of pure g-C_3N_4 appears at about 440 nm, which is in accordance with the bandgap of g-C_3N_4. This strong peak is

attributed to the n→π* electronic transition involving lone pairs of nitrogen atoms in g-C_3N_4.[21] In comparison with the g-C_3N_4, the intensity of the PL signal for the g-C_3N_4/NiO obviously decreased. This demonstrates that the recombination of photogenerated electrons and holes is greatly inhibited, which indicates that the excited electrons can transfer between the g-C_3N_4 and NiO.[31, 37, 46]

Electrochemical impedance spectroscopy (EIS) was employed to examine the electron transfer process occurring among the g-C_3N_4/NiO catalysts and the protons. Fig. 6(b) showed EIS results presented in the form of Nyquist plots. These three electrodes were measured under the same conditions. The overall HER activity can be related to the charge transfer resistance (R_{ct}). The charge transfer resistance (R_{ct}) across the interface of the semiconductor electrode and the electrolyte was determined from the semicircle in the low-frequency range. As can be seen, g-C_3N_4/NiO composite electrode exhibited smallest R_{ct} than the NiO electrode and g-C_3N_4 electrode, indicating the more favorable environment for electron transfer to the electrolyte. Thus the combination of g-C_3N_4 and NiO lowers the recombination rate of electrons and holes, which is mainly due to the fact that the electrons are excited from the valence band to the conduction band and then holes appears at the valence band can be transfer rapidly to NiO, preventing a direct recombination of electrons and holes. In addition, the R_{ct} of g-C_3N_4 was smaller than that of NiO, so it can help release photogenerated electrons accumulated on the surface of g-C_3N_4 itself as a co-catalyst. From

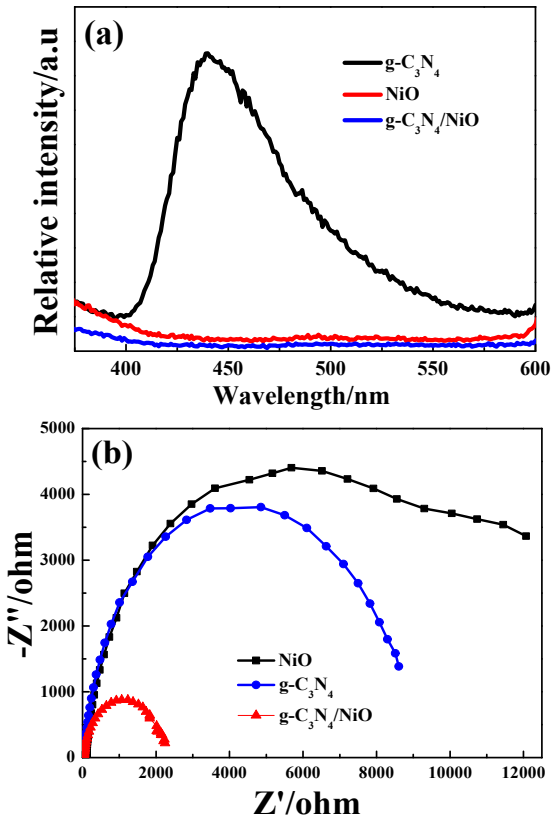

Figure 6. (a) Photoluminescence spectra of the g-C_3N_4, NiO electrode and g-C_3N_4/NiO electrode; (b)Nyquist plots for the g-C_3N_4/FTO, NiO/FTO and g-C_3N_4/NiO/FTO electrodes in 0.10 M Na_2SO_4 solution.

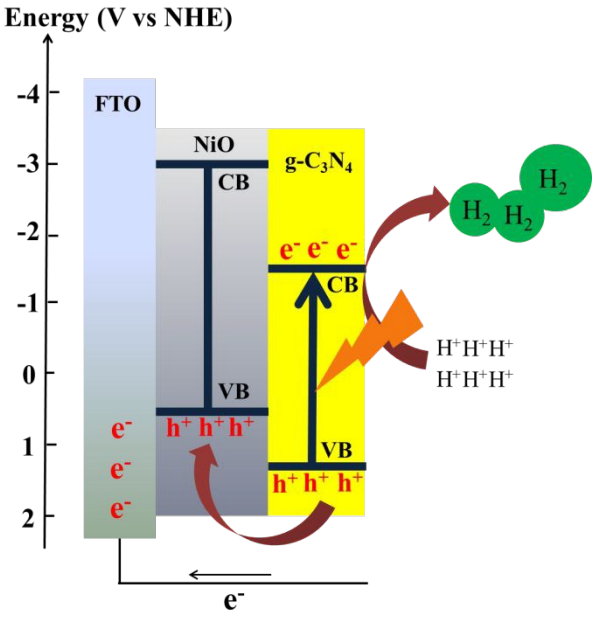

Figure 7. The mechanism of PEC H_2 generation using g-C_3N_4/NiO electrode.

above analysis, we know that g-C_3N_4 can not only be used as a photosensitizer absorbs sunlight but also enhance the reactivity as a co-catalyst in PEC hydrogen production.

Based on the results of PEC tests, PL and EIS analysis of the as-prepared electrodes, a possible mechanism is proposed and shown in Fig. 7. The significant enhancement of PEC performance can be attributed to synergistic effect between g-C_3N_4 and NiO. The bandgap of g-C_3N_4 is determined to be 2.85 eV, while lowest unoccupied molecular orbital (LUMO) and highest occupied molecular orbital (HOMO) positions of g-C_3N_4 are −1.58 and 1.27 eV, respectively.[30] The HOMO poten-tial of g-C_3N_4 is more positive than the conduction band (VB) edge of NiO (0.6 eV).[45] Upon irradiation on g-C_3N_4/NiO, g-C_3N_4 itself becomes excited by creating reductive electrons and oxidative holes in the CB and VB, respectively, and NiO is hardly excited because it is a wide band gap semiconductor. The oxidative holes in the VB of g-C_3N_4 can directly inject into the VB of NiO, and be consumed by the electrons from external circuit. At the same time, the reductive electrons can directly produce hydrogen to react with H^+ in electrolyte thereby leading to the reduction of electron-hole pair recombination. The matching potential between g-C_3N_4 and NiO is a driving force for the holes transfer. Thus, the recombination of electrons and holes can be suppressed. Further, under an applied potential, an external electric field between the two semiconductors will form, thus enhances the transfer and separation of photoinduced electrons and holes.

4. Conclusions

In summary, we have synthesized a novel photocathode based on g-C_3N_4 by a facile thermalpolycondenzation method. The photoelectrochemical properties of the prepared electrodes were systematically investigated. The synergistic effect between g-C_3N_4

and NiO contributed significantly to the enhancement of PEC performance. Therefore, the g-C_3N_4/NiO photoelectrode has excellent activity for hydrogen production with nearly 100% faraday efficiency compared to bare g-C_3N_4 and NiO electrodes. Moreover, the g-C_3N_4/NiO photoelectrode maintains high stability in presence and absence of oxygen during 10 h and can be applicable in wide electrolyte solution. There are few studies on g-C_3N_4 as metal-free photosensitizer for photocathode, so it has great space for development. That will enrich the variety of existing photocathode and would pave the way toward the investigations of non-toxic, metal-free and stable photocathode.

Acknowledgements

The authors gratefully acknowledge the support from the National Natural Science Foundation of China (No. 21575052, 21275065), the Fundamental Research Funds for the Central Universities (JUSRP51507), MOE & SAFEA for the 111 Project (B13025).

Notes and references

1 A. Kudo, Y. Miseki, *Chem. Soc. Rev.*, 2009, **38**, 253-278.
2 Y. P. Hu, X. Q. Yan, Y. S. Gu, X. Chen, Z. M. Bai, Z. Kang, F. Long and Y. Zhang, *Appl. Surf. Sci.*, 2015, **339**, 122-127.
3 Z. S. Li, W. J. Luo, M. L. Zhang, J. Y. Feng and Z. G. Zou, *Energy Environ. Sci.*, 2013, **6**, 347-370.
4 M. Shalom, S. Gimenez, F. Schipper, I. Herraiz-Cardona, J. Bisquert, M. Antonietti, *Angew. Chem. Int. Ed.*, 2014, **53**, 3654-3658.
5 M. J. Kenney, M. Gong, Y. G. Li, J. Z. Wu, J. Feng, M. Lanza and H. J. Dai, *Science*, 2013, **342**, 836-840.
6 T. J. Jacobsson, V. Fjällström, M. Edoff and T. Edvinsson, *Energy Environ. Sci.* 2014, **7**, 2056-2070.
7 M. I. Asghar, K. Miettunen, J. Halme, P. Vahermaa, M. Toivola, K. Aitola and P. Lund, *Energy Environ. Sci.*, 2010, **3**, 418-426.
8 L. Li, L. Duan, F. Y. Wen, C. Li, M. Wang, A. Hagfeldt and L. C. Sun, *Chem. Commun.*, 2012, **48**, 988-990.
9 Z. Q. Ji, M. F. He, Z. J. Huang, U. Ozkan, Y and Y Wu, *J. Am. Chem. Soc.*, 2013, **135**, 11696-11699.
10 G. Ai, W. T. Sun, X. F. Gao, Y. L. Zhang and L. M. Peng, *J. Mater. Chem.*, 2011, **21**, 8749-8755.
11 Z. Han, F. Qui, R. Eisenberg, P. L. Holland and T. D. Krauss, *Science*, 2012, **338**, 1321-1324.
12 M. B. Wilker, K. E. Shinopoulos, K. A. Brown, D. W. Mulder, P. W. King and G. Dukovic, *J. Am. Chem. Soc.*, 2014, **136**, 4316-4324.
13 B. C. M. Martindale, G. A. M. Hutton, C. A. Caputo and E. Reisner, *J. Am. Chem. Soc.*, 2015, **137**, 6018-6025.
14 J. S. Zhang, G. G. Zhang, X. F. Chen, S. Lin, L.; Dołega, G. Mohlmann, G. Lipner, M. Antonietti, S. Blechert and X. C. Wang, *Angew. Chem. Int. Ed.*, 2012, **51**, 3183-3187.
15 Y. Y. Bu, Z. Y. Chen and W. B. Li, *Appl. Catal. B: Environ.*, 2014, **144**, 622-630.
16 J. Xu, H. T. Wu, X. Wang, B. Xue, Y. X. Li and Y. Cao, *Phys. Chem. Chem. Phys.*, 2013, **15**, 4510-4517.
17 S. Z. Hu, L. Ma, J. G. You, F. Y. Li, Z. P. Fan, G. Lu, D. Liu and J. Z. Gui, *Appl. Surf. Sci.*, 2014, **311**, 164-171.
18 H. Zhao, Y. M. Dong, P. P. Jiang, H. Y. Miao, G. L. Wang and J. J. Zhang, *J. Mater. Chem. A*, 2015, **3**, 7375-7381.
19 D. J. Martin, P. J. T. Reardon, S. J. A. Moniz and J. W. Tang, *J. Am. Chem. Soc.*, 2014, **136**, 12568-12571.
20 J. H. Liu, Y. W. Zhang, L. H. Lu, G. Wu, W. Chen, *Chem. Commun.*, 2012, **48**, 8826-8828.
21 Q. J. Xiang, J. G. Yu and M. Jaroniec, *J. Phys. Chem. C*, 2011, **115**, 7355-7363.
22 J. D. Hong, Y. S. Wang, Y. B. Wang, W. Zhang and R. Xu, *ChemSusChem*, 2013, **6**, 2263-2268.
23 W. B. Li, C. Feng, S. Y. Dai, J. G. Yue, F. X. Hua and H. Hou, *Appl. Catal. B-Environ.*, 2015, **168-169**, 465-471.
24 C. Han, Y. D. Wang, Y. P. Lei, B. Wang, N. Wu, Q. Shi and Q. Li, *Nano Res.*, 2015, **4**, 1199-1209.
25 Z. Y. Wang, W. Guan, Y. J. Sun, Fan. Dong, Y. Zhou and W. K. Ho, *Nanoscale*, 2015, **7**, 2471-2479.
26 X. H. Zhang, L. J. Yu, C. S. Zhuang, T. Y. Peng, R. J. Li and X. G. Li, *ACS Catal.*, 2014, **4**, 162-170.
27 B. Chai, T. Y. Peng, J. Mao, K. Li and L. Zan, *Phys. Chem. Chem. Phys.*, 2012, **14**, 16745-16752.
28 K. Schwinghammer, M. B. Mesch, V. Duppel, C. Ziegler, J. Senker and B. V. Lotsch, *J. Am. Chem. Soc.*, 2014, **136**, 1730-1733.
29 K. Tian, W. J. Liu and H. Jiang, *ACS Sustainable Chem. Eng.*, 2015, **3**, 269-276.
30 F. He, G. Chen, Y. G. Yu, S. Hao, Y. S. Zhou and Y. Zheng, *ACS Appl. Mater. Interfaces*, 2014, **6**, 7171-7179.
31 M. A. Gondal, A. A. Adesida, S. G. Rashid, S. Shi, R. Khan, Z. H. Yamani, K. Shen, Q. Y. Xu, Z. S. Seddigi and X. F. Chang, *Reac. Kinet. Mech. Cat.*, 2015, **114**, 357-367.
32 B. Yuan, Z. Y. Chu, G. Y. Li, Z. H. Jiang, T. J. Hu, Q. H. Wang and C. H. Wang, *J. Mater. Chem. C*, 2014, **2**, 8212-8215.
33 H. J. Li, B. W. Sun, L. Sui, D. J. Qian and M. Chen, *Phys. Chem. Chem. Phys.*, 2015, **17**, 3309-3315
34 Liu, J.; Liu, Y.; Liu, N. Y.; Han, Y. Z.; Zhang, X.; Huang, H.; Lifshitz, Y.; Lee, S. T.; Zhong, J.; Kang, Z. H. Metal-Free Efficient Photocatalyst for Stable Visible Water Splitting via a Two-Electron Pathway. Science **2015**, 6225, 970-974.
35 J. J. Duan, S. Chen, M. Jaroniec and S. Z. Qiao, *ACS Nano.*, 2015, **9**, 931-940.
36 B. B. Wang, H. T. Yu, X. Quan and S. Chen, *Mater. Res. Bull.*, 2014, **59**, 179-184.
37 J. Wang, F. Y. Su and W. D. Zhang, *J. Solid State Electrochem.*, 2014, **18**, 2921-2929.
38 J. R. Manders, S. W. Tsang, M. J. Hartel, T. H. Lai, S. Chen, C. M. Amb, J. R. Reynolds and F. So, *Adv. Funct. Mater.*, 2013, **23**, 2993-3001.
39 Z. C. Zhai, X. D. Huang, M. F. Xu, J. Y. Yuan, J. Peng and W. L. Ma, *Adv. Energy Mater.*, 2013, **3**, 1614-1622.
40 T. P. A. Ruberu, Y. M. Dong, A. Das and R. Eisenberg, *ACS Catal.*, 2015, **5**, 2255-2259.
41 B. Liu, X. B. Li, Y. J. Gao, Z. J. Li, Q. Y. Meng, C. H. Tung and L. Z. Wu, *Energy Environ. Sci.*, 2015, **8**, 1443-1449.
42 H. Y. Chen, L. G. Qiu, J. D. Xiao, S. Ye, X. Jiang and Y. P. Yuan, *RSC Adv.*, 2014, **4**, 22491-22496.
43 X. C. Wang, K. Maeda, A. Thomas, K. Takanabe, G. Xin, J. M. Carlsson, K. Domen and M. Antonietti, *Nat. Mater.*, 2009, **8**, 76-80.
44 V. Biju. *Mater. Res. Bull.*, 2007, **42**, 791-796.
45 Y. M. Dong, Y. M. Chen, P. P. Jiang, G. L. Wang, X. M. Wu, R. X. Wu and C. Zhang, *Chem. Asian J.*, 2015, **8**, 1660-1667.

46 X. H. Zhang, T. Y. Peng, L. J. Yu, R. J. Li, Q. Q. Li, Z. Li, *ACS Catal.*, 2015, **5**, 504-510.

FOR TABLE OF CONTENTS ENTRY USE

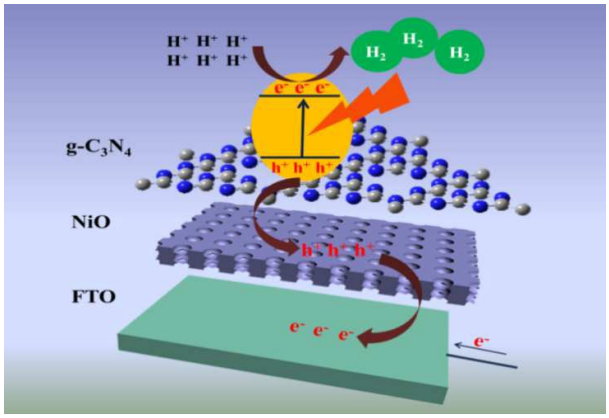

Title: *A Novel g-C_3N_4 Based Photocathode for Photoelectrochemical Hydrogen Evolution*

Authors: *Yuming Dong*, Yanmei Chen, Pingping Jiang, Guangli Wang, Xiuming Wu and Ruixian Wu*

Synopsis: *Novel and stable g-C_3N_4 based photocathode was designed and prepared with excellent activity for PEC hydrogen production without external co-catalyst.*